Supporting Information

With respect to the Ag NPs immobilized on the AAO surface, as shown in the left and middle column in Fig. S1, those situated close to each other on the surface began to coalesce to form larger Ag NPs after annealing for 20 min. Fusion continued for the Ag NPs treated for 60 min and 180 min but with far more coalescence to form single large Ag particles. Note that micro-scale structural features were formed and grew larger as annealing time increased, stemming from clustering of Ag NPs. Note that many small Ag NPs could still be found on the surface of AAO after annealing for up to 5 days. In contrast, as shown in the right column in Fig. S1, coalescence of Ag NPs was limited and a uniform distribution of small Ag NPs was preserved inside the AAO channels. This observation is in stark contrast with what was seen for Ag NPs on the AAO surface, a strong indication that nanoporous AAO physically mitigates the fusion and evaporation of Ag NPs inside the pores. Corresponding SERS measurements are reported in Fig. S2. Comparable SERS intensities of Ag NPs prior to annealing and after annealing for 20, 60, 180, and 360 min were observed. Note that the overlapping background in the same range (1200-1800 cm^{-1}) as the R6G feature peaks is attributed to the organic polymer cluster formed upon heating on the AAO surface as shown in Fig. S1. As the annealing time increases to 1 day and 5 days, the Raman intensity underwent a striking drop due to lack of "hot spots" from insufficient amount of Ag NPs caused by significant evaporation depletion.

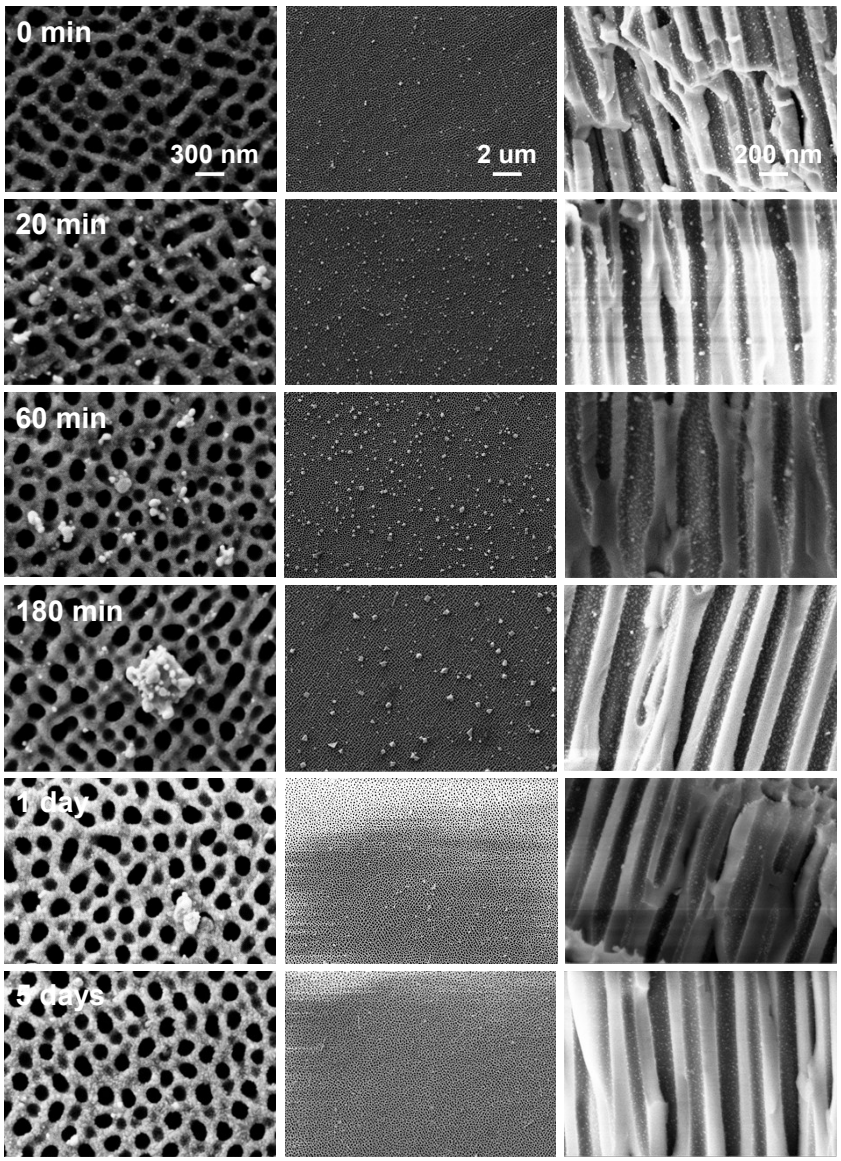

Figure S1. SEM images of *in-situ* growth of Ag NPs inside AAO structure without annealing and after annealing at 500°C for 20 min, 60 min, 180 min, 1 day, and 5 days respectively. Plan-view with (Left) 100 kX and (Middle) 10 kX magnification, and (Right) cross-section view for each annealing time are illustrated.

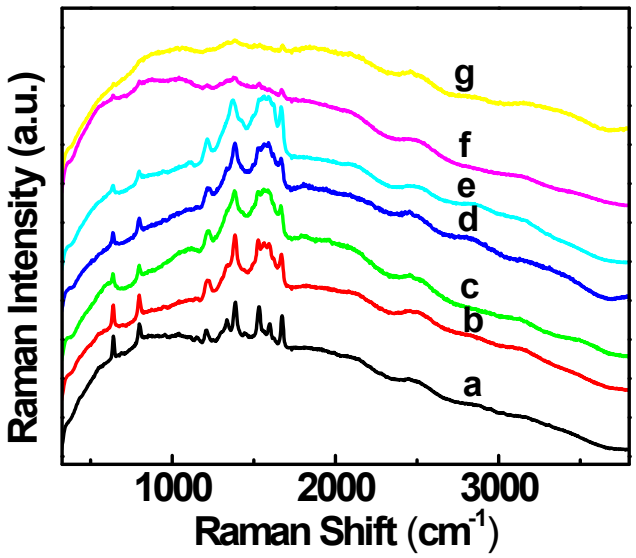

Figure S2. Raman spectra of 10^{-5} M R6G solution of Ag NPs inside AAO (a) before and after annealing for (b) 20 min, (c) 60 min, (d) 180 min, (e) 360 min, (f) 1 day, and (g) 5 days, respectively.

A similar morphological trend, compared to that for 500°C (see Fig. S1), was observed for the Ag NPs on the AAO surface upon heating at 600°C except for the formation and then disappearance of large particle clusters within the first hours, as shown in the left and middle column in Fig. S3. As shown in the right column in Fig. S3, coalescence of Ag NPs in close proximity did occur during the early stages of annealing treatment, leading to markedly increased particle size. A statistically uniform distribution of Ag NPs with a gradual reduction in particle size due to mass loss from evaporation remains the prevailing feature inside the AAO pore channels. Corresponding Raman measurements indicated the SERS ability of the Ag NPs after annealing for 20, 60, and 180 min, but not for 1 day and 5 days.

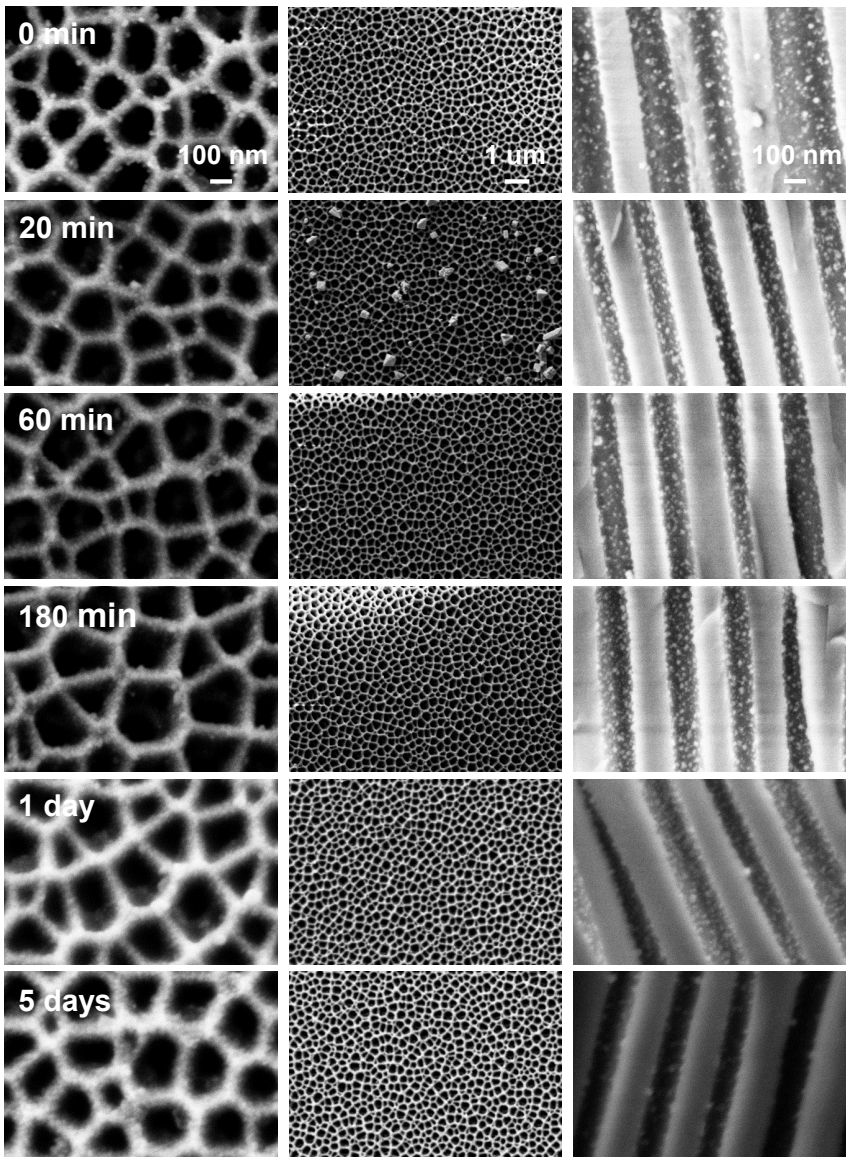

Figure S3. SEM images of in situ growth of Ag NPs inside AAO structure without annealing and after annealing at 600°C for 20, 60, 180 min, 1 day, and 5 days, respectively. Plan-view with (Left) 200 kX (Middle) 33 kX magnification and (Right) cross-section view for each annealing time are illustrated.

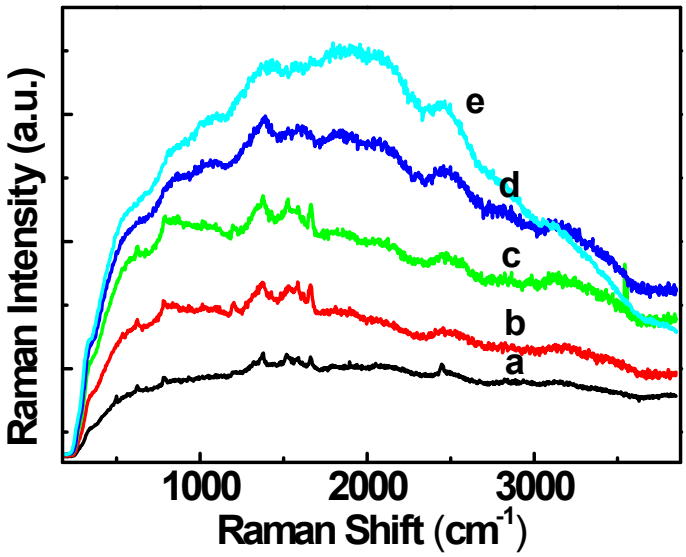

Figure S4. Corresponding Raman spectra of 10^{-6} M R6G of Ag NPs inside AAO after annealing for (a) 20 min, (b) 60 min, (c) 180 min, (d) 1 day, and (e) 5 days, respectively.

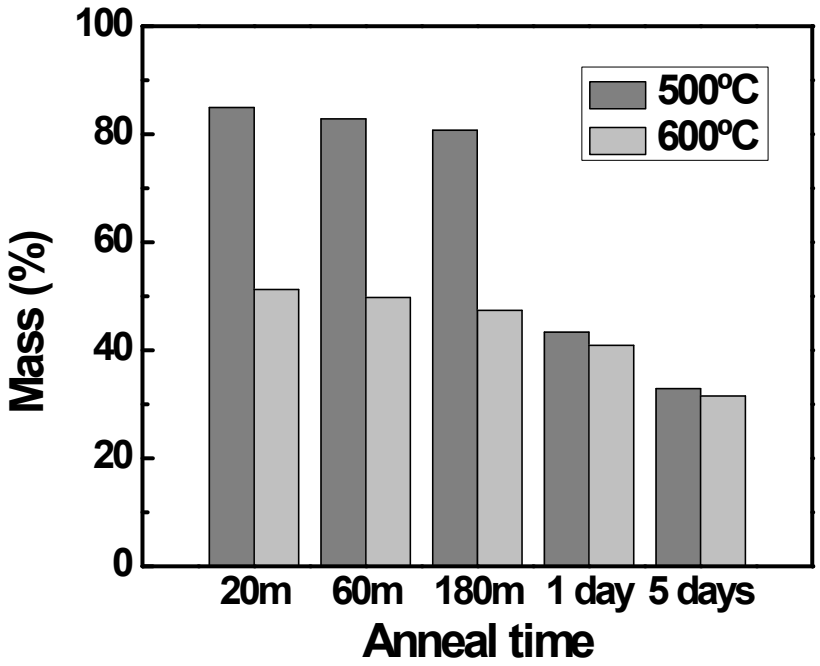

Figure S5. Mass percentage of the total amount of annealed Ag NPs in the pore channels of AAO as compared to that before annealing.

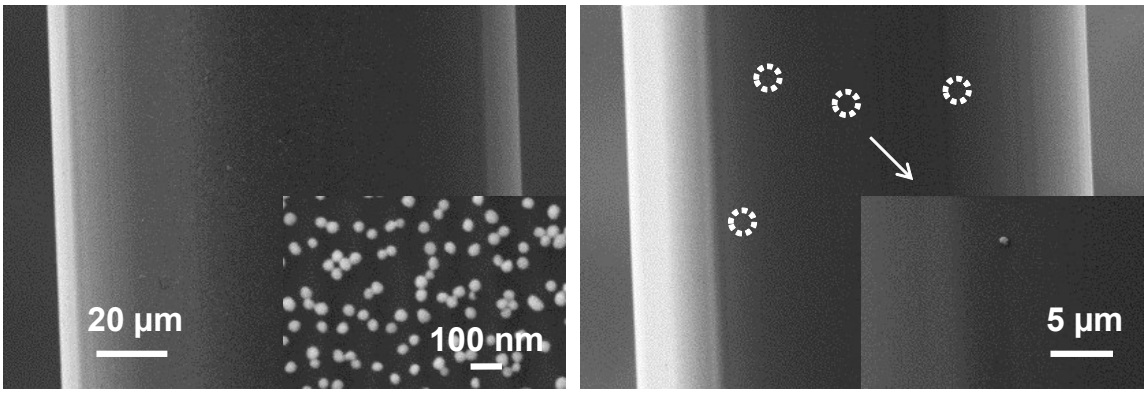

Figure S6. SEM microscopy images of Ag NPs immobilized on the surface of sapphire (Al_2O_3) optical fiber before (left) and after (right) annealing at 500°C for 6 hr.

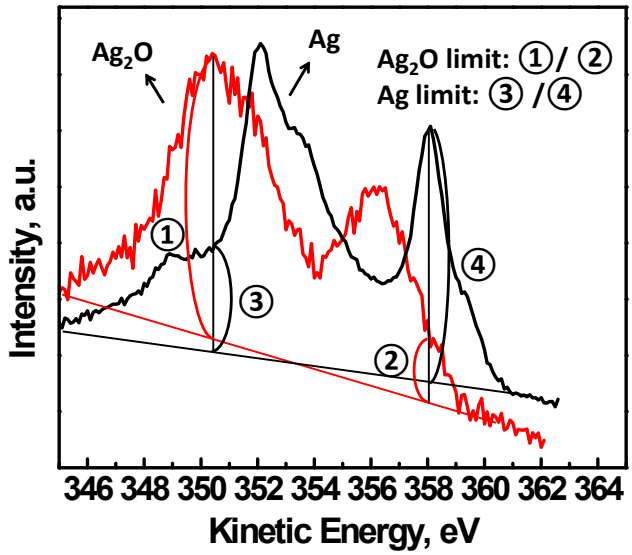

Figure S7. The calculation method for the pure Ag and Ag_2O limits shown in Fig. 6 in the manuscript. Black and red curve relates to the Auger spectra of metallic Ag and Ag_2O. The intensity ratio between the spectrum of Ag_2O and its straight baseline (in red) at a kinetic energy of 350.5 eV (main peak of Ag_2O) and 358.1 eV (main peak of Ag) is defined as Ag_2O limit: ①/②. The intensity ratio between the spectrum of Ag and its straight baseline (in black) at a

kinetic energy of 350.5 eV (main peak of Ag_2O) and 358.1 eV (main peak of Ag) is defined as Ag limit: ③/④.

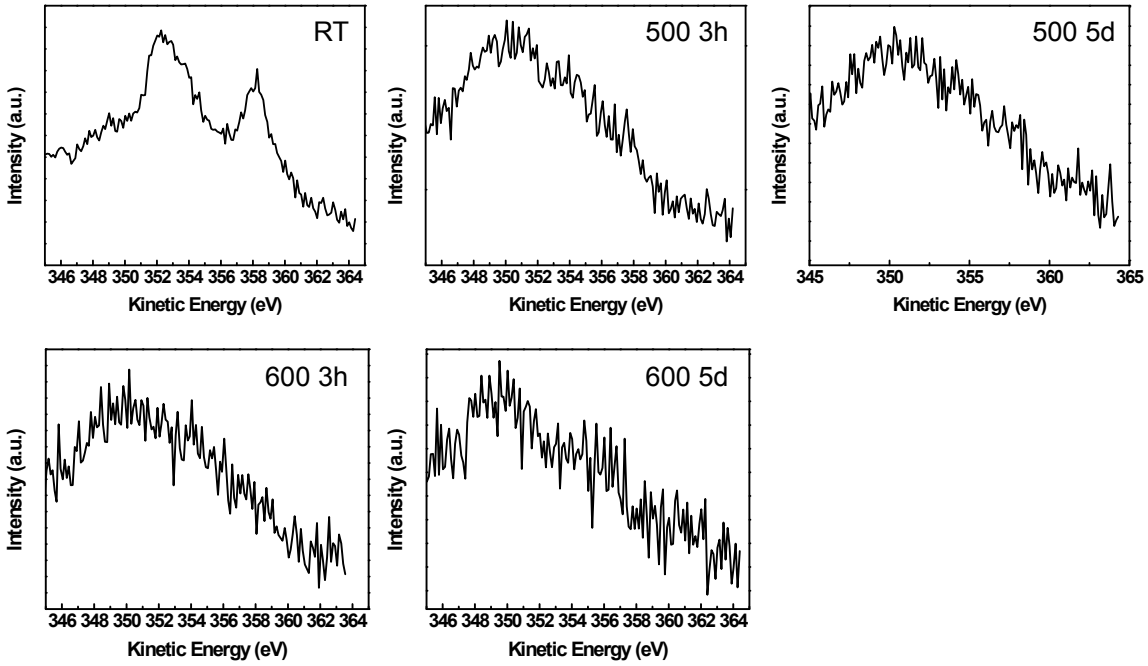

Figure S8. Auger peak of Ag NPs on the AAO surface before and after various heat treatments.

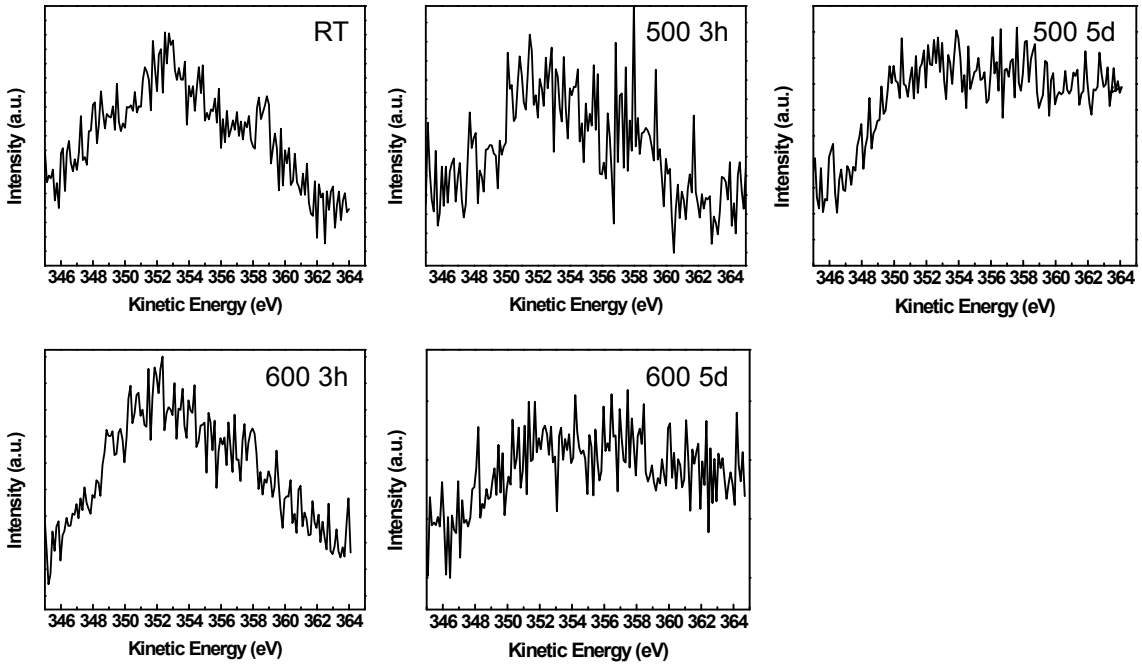

Figure S9. Auger peak of Ag NPs inside AAO before and after various heat treatments.

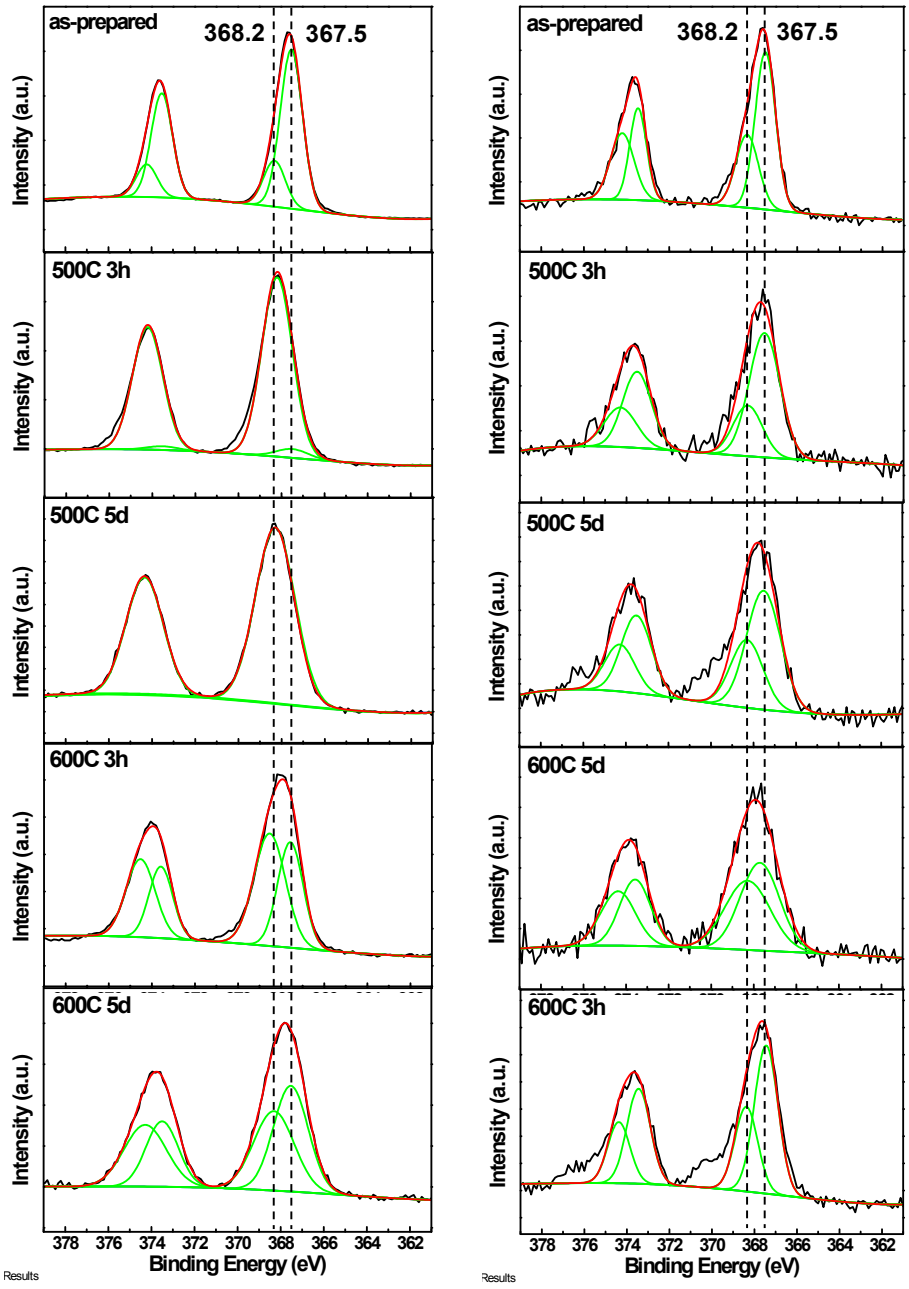

Figure S10. Curve fitted Ag $3d_{5/2}$ peak (left column) on the AAO surface and (right column) inside AAO before and after various heat treatments. The raw data (in black), the cumulative fitted curves (in red), and all the four fitted peaks at the binding energies of 374.2, 373.5, 368.2, 367.5 eV (in green) for Ag $3d_{3/2}$ and $3d_{5/2}$ peaks are illustrated. All the four fitted peaks in each spectrum have the same full width at half maximum (FWHM).

The enhancement factor (EF) was calculated using $EF = (I_{SERS}/C_{SERS})/(I_{NR}/C_{NR})$, where I_{SERS} and I_{NR} are the integrated intensities of a characteristic band from SERS and from normal Raman (normalized for acquisition time and laser power), and C_{SERS} and C_{NR} are concentrations of analytes used in SERS and normal Raman experiments, respectively. The feature peak of R6G at a wavelength of 1360 cm^{-1} was selected as the characteristic band for calculation. The respective concentrations of R6G analyte were chosen at 10^{-6} and 10^{-3} M for SRES and normal Raman measurements. I_{SERS} is estimated at 889470, 764944, and 373577 for curve a, b, and c, respectively, while I_{NR} is estimated at 1779, by calculating the integrating areas of peak at 1360 cm^{-1} using Origin 8.5. C_{SERS} and C_{NR} are defined as 10^{-6} and 10^{-3} M. Therefore, according to equation $EF = (I_{SERS}/C_{SERS})/(I_{NR}/C_{NR})$, SERS EFs for curve a, b, and c are obtained as 2.1×10^5, 4.3×10^5, and 5.0×10^5, respectively.

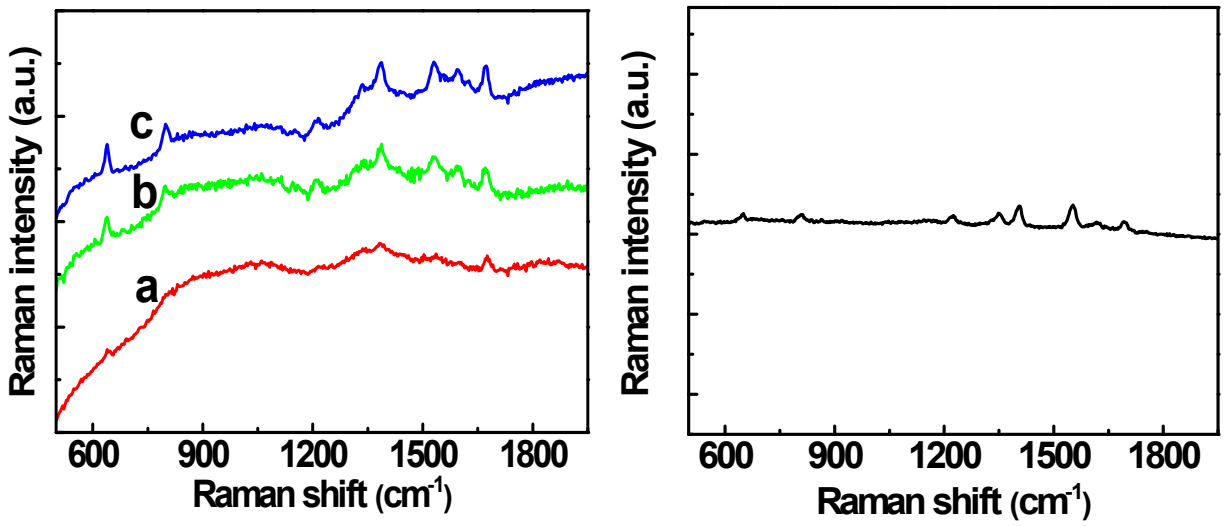

Figure S11. (Left) SERS and (Right) normal Raman spectra of 10^{-6} and 10^{-3} M R6G analyte, respectively, for silver nanoparticles entrapped within AAO pore channels (SEM images are shown in Fig. 1). Curve a, b, c in the left graph (same as shown in Fig. 2) represents the SERS

spectra using *in-situ* grown Ag NPs with 10.3±3.1, 13.3±4.7, 15.6±5.6 nm in diameter, respectively.